BALKAN PHYSICS LETTERS
©Bogazici University Press 15 June 2014
BPL, 22, 221013, pp. 119 – 128, (2014)

PREPARATION OF CUBIC ROCK SALT LEAD SULFIDE THIN FILMS AND THE STUDY OFTHEIR MICROSTRUCTURE AND OPTICAL PROPERTIES

F. GODE
Physics Department, Mehmet Akif Ersoy University,
Burdur, TURKEY.

S. CEVIK
Physics Department, Mehmet Akif Ersoy University,
Burdur, TURKEY.

E. GUNERI
Primary Education Department, Erciyes University,
Kayseri, TURKEY.

and

S. UNLU
Physics Department, Mehmet Akif Ersoy University,
Burdur, TURKEY.

Abstract. Lead sulfide thin films with three different concentrations of cationic precursor as 0.04 M, 0.05 M and 0.06 M were prepared by successive ionic layer adsorption and reaction method on glass substrates at room temperature. The structural, morphological, compositional and optical properties of the films have been investigated by means of room temperature x-ray diffraction, scanning electron microscope, energy dispersive analysis by x-rays and transmittance and absorption spectral analysis, respectively. The x-ray diffraction technique has shown that all films have a polycrystalline of a cubic rock salt unit cell that exhibit the lattice parameter of $a \approx$ 0.596 nm. The optical parameters of the films such as the refractive index, extinction coefficient, real and imaginary part of the dielectric constants were calculated from the absorbance and transmittance data. Moreover, the optical band gap of the films decreased from 2.68 eV to 2.58 eV with increasing cationic precursor concentration.

1. INTRODUCTION

Lead sulfide (PbS) has a cubic crystal structure and a narrow direct band gap, small effective mass and high electron mobility. Its band gap can be varied in a wide range, up to 2.3 eV, from the bulk value of 0.41 eV, by changing the mean cluster size of the nanoclusters [1]. It permits size quantization effects to be clearly seen even for large particles or crystallites, and make it an interesting system for studying the effects of size confinement [2]. PbS widely used in many fields such as in thin film transistors (TFTs) [3], light-emitting diodes [4], IR detectors [5] and solar cells [6].

These films can be obtained by several methods such as electrodeposition [7], solvothermal [2], microwave and sonochemical [8], microwave-assisted heating [9], successive ionic layer absorption and reaction (SILAR) [10] and chemical bath deposition (CBD) [11]. Among them, SILAR is one of the chemical techniques for producing metal chalcogenide films. In this method, the films were deposited by alternately dipping of a substrate into the aqueous solutions containing ions of each component. The growth mechanism and the thickness of the films deposited depend on several factor, the temperature and concentration of the solution, nature of the substrate, immersion time in respective precursor solution, precursor pH and subsequent rinsing time in deionized water, etc. Thin film deposition occurs by a chemical reaction between the chalcogen ions in solution and the adsorbed metal ions on substrate.

PbS is the one of the most important IV-VI semiconductor compound used in optoelectronic devices. So, the knowledge of the crystallographic, surface morphology, optical and electrical properties of PbS films is necessary for the design and manufacture of these devices. This paper presents our observations of cationic precursor effects on the formation of PbS thin films and their optical parameters.

2. EXPERIMENTAL DETAILS

In order to produce PbS thin films, three different lead acetate concentration of 0.04 M, 0.05 M and 0.06 M were used as cationic precursor and the anionic concentration of thioacetamide was kept invariant at 0.06 M. The pH of the cationic and anionic solution was adjusted to ~9.66 and ~10.48 by adding ammonia (NH_3) drop by drop, respectively. Glass substrates immersed into cationic precursor solution for 20 s, and then rinsed with deionized water for 40 s to remove the unattached ions. Then the substrate immersed into anionic precursor for another 20 s and rinsed again in the deionized water for 40 s to complete one full cycle of operation. The dipping cycle was repeated 25 times. Produced films were dried in even at 60 °C. The colors of the films changed from light grey to dark grey with increasing cationic precursor concentration.

3. RESULTS AND DISCUSSION

The x-ray powder diffraction patterns for PbS films with three different cationic precursor concentration obtained by using Cu$K\alpha$ radiation, are shown in figure 1. The diffraction data (the peak positions and intensities) of the films indicate the existence of cubic rock-salt (NaCl) structure (PDF

card No. 05-0592; a = 0.594 nm) with four diffraction peaks corresponding to (111), (200), (220) and (311) planes. The x-ray data for the PbS films of the diffraction lines are presented in table 1.

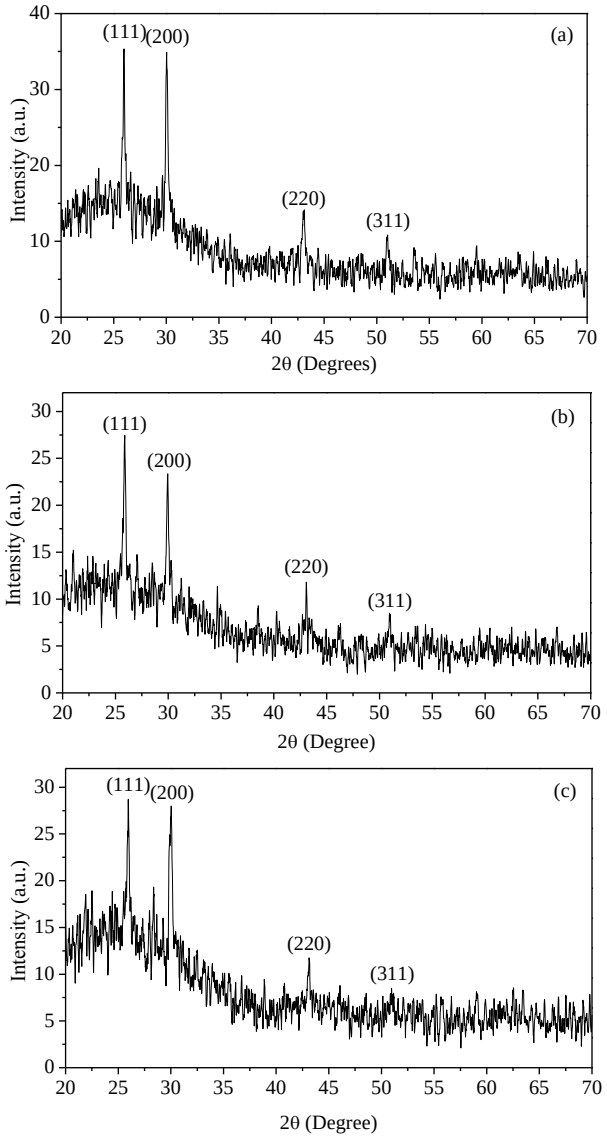


Figure 1: XRD patterns of PbS thin films grown with different cationic precursor concentration (a) 0.04 M, (b) 0.05 M and (c) 0.06 M.

Table 1: The plane indices (*hkl*), Bragg angle (2θ), length between planes (d), grain size (D), and lattice parameter (a) for the PbS films with various concentrations of cationic precursor.

Pb concentration (M)	*hkl*	2θ (°) Observed	d (nm) Observed	2θ (°) Standard	d (nm) Standard	D (nm)	a (nm)
0.04	111	25.825	0.3447	25.964	0.3429	47	5.97
	200	30.065	0.2970	30.075	0.2969	36	5.94
	220	43.096	0.2097	43.059	0.2099	19	5.94
0.05	111	25.825	0.3447	25.964	0.3429	40	5.97
	200	29.948	0.2981	30.075	0.2969	40	5.96
	220	43.096	0.2097	43.059	0.2099	59	5.94
0.06	111	25.942	0.3432	25.964	0.3429	15	5.94
	200	30.026	0.2974	30.075	0.2969	25	5.94
	220	43.057	0.2091	43.059	0.2099	24	5.94

The lattice parameter was calculated using the d value (inter-planar spacing) for the cubic structure, which is given by [12]:

$$a = d\sqrt{h^2 + k^2 + l^2} \qquad (1)$$

where (*hkl*) is the Miller indices of the plane concerned and a is the lattice parameter. The value of the lattice parameter of the PbS films have been found to be $a \approx 0.596$ nm, which is in good agreement with the standard value of the lattice parameter taken from PDF card file data (the reference data for the bulk galena crystals is $a = 0.594$ nm) (table 1). The crystallite sizes have been evaluated using the Scherrer formula [13]:

$$D = \frac{0.9\lambda}{\beta cos\theta} \qquad (2)$$

where λ is the wavelength of the x-ray, θ is the Bragg angle and β is the width of half maxima. As seen from the table 1, the average crystallite size of the film grown at 0.05 M cationic precursor was calculated to be 40 nm for the observed (200) diffraction peak.

Scanning electron microscopy (SEM) studies were performed using a EVO40-LEO model. The SEM micrographs of the films show the good coverage of the substrate with small spherical shape in figure 2. In order to determine the chemical composition of the PbS films, energy dispersive X-ray spectrometry (EDX) was carried out. The stoichiometric ratios for all films are found to be 0.82, 0.53 and 0.92 for 0.4 M, 0.5 M and 0.6 M cationic precursor concentration, respectively. It can be seen that the film obtained at 0.6 M cationic precursor seems more stoichiometric than the others.

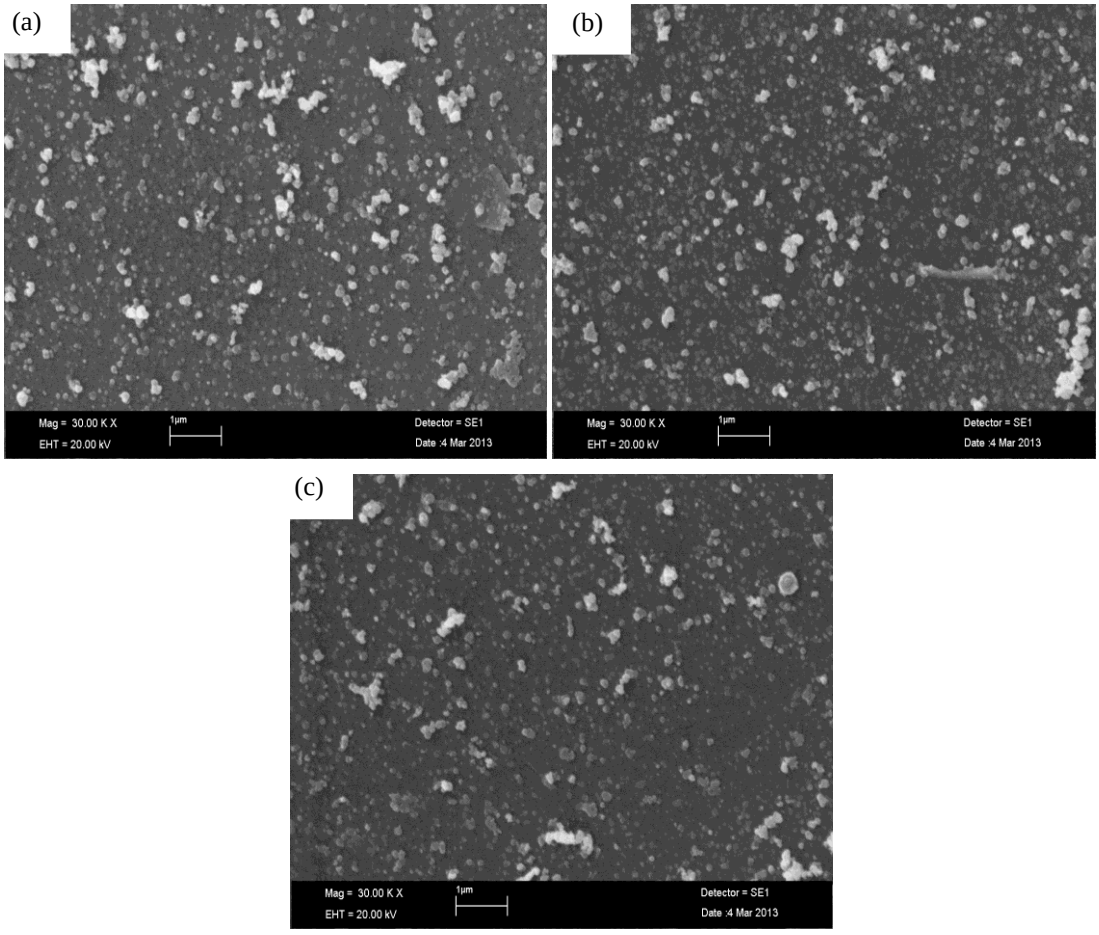


Figure 2: SEM micrographs for PbS films with different cationic precursor concentration (a) 0.04 M, (b) 0.05 M and (c) 0.06 M.

The thicknesses of the films between 607 nm and 732 nm are determined by the weight difference method assuming that the sample is uniform and dense as that of the bulk having a density of 7.597 g cm^{-3} in table 3.

Table 2: EDX analysis for PbS thin films with various cationic precursors concentration

Pb concentration (M)	Element (%)		S/Pb
	S	Pb	
0.04	3.22	3.94	0.82
0.05	1.87	3.54	0.53
0.06	3.10	3.38	0.92

Table 3: A summary of the thicknesses and optical parameters of PbS films with different cationic precursor concentration (λ = 600 nm)

Pb concentration (M)	*t* (nm)	*n*	*k*	ε_1	ε_2	E_g (eV)
0.04	607	4.41	0.90	18.60	7.94	2.68
0.05	676	4.76	0.88	21.92	8.38	2.63
0.06	732	5.81	1.01	32.71	11.75	2.58

UV-Vis transmission spectra were recorded in the 400–1100 nm on a Perkin Elmer Lambda 2S spectrophotometer, shown in figure 3. It is seen from this figure 3(a) that the transparency of the deposited film decreased from ~7% to ~3% with the increase of cationic precursor concentration at 600 nm wavelength in the visible region. The reflectivity of the material having refractive index (*n*) and extinction coefficient (*k*) is given by [14]:

$$R = \frac{(n-1)^2 + k^2}{(n+1)^2 + k^2} \qquad (3)$$

The transmittance is represented by the relation:

$$T = \frac{(1-R)^2 \exp(-\alpha t)}{1 - R^2 \exp(-2\alpha t)} \qquad (4)$$

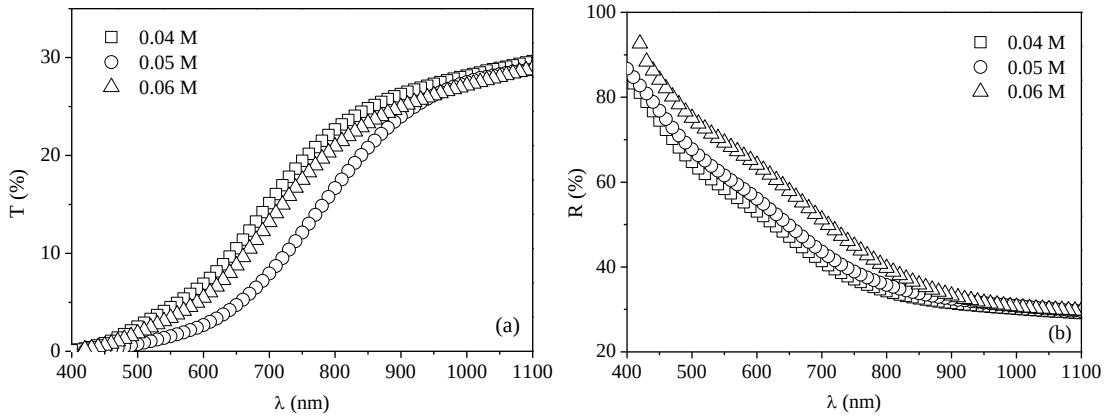


Figure 3: (a) Transmission and (b) reflectance curves for PbS thin films.

where α is the absorption coefficient and t is the film thickness. α is related to k by the expression $\alpha = 4\pi k/\lambda$. With the help of the above relations, the optical constants refractive index (n), extinction coefficient (k), can be calculated from the absorbance, reflectivity and transmittance measurements. Figure 4 demonstrates the spectral dependences of refractive index and extinction coefficient, calculated by means of equations (3) and (4). As listed in table 3, refractive index and extinction coefficient for the PbS film increased from 4.41 to 5.81 and from 0.90 to 1.01 at λ = 600 nm wavelength with the increase in cationic precursor concentration, respectively. It can be said that our refractive index value is consistent with other works [15-17].

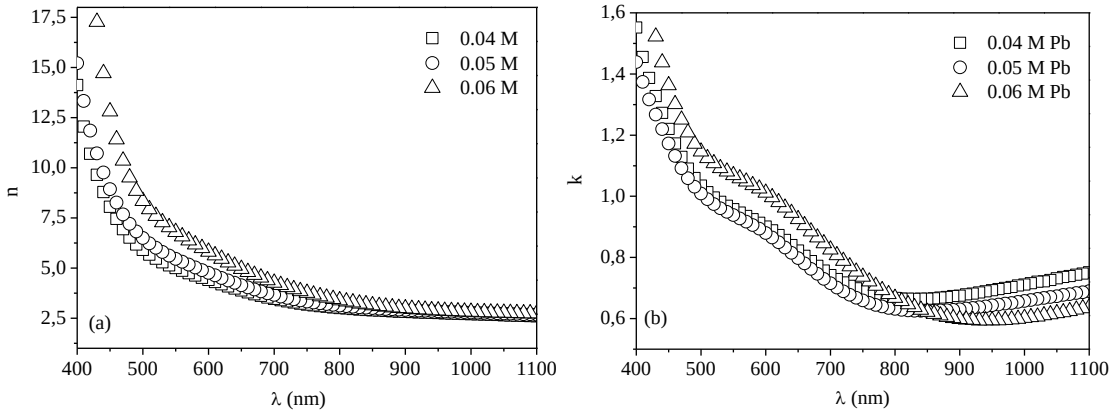


Figure 4: The spectral dependences of (a) refractive index and (b) extinction coefficient for the PbS thin films.

It is well known that polarizability of any solid is proportional to its dielectric constant. The real and imaginary parts of the complex dielectric constant are calculated using the following equations [18]:

$$\varepsilon_1 = n^2 - k^2 \qquad (5)$$

$$\varepsilon_2 = 2nk \qquad (6)$$

where ε_1 is the real part and ε_2 is the imaginary part of the dielectric constant. The real and imaginary parts of the dielectric constant were calculated by using n and k values from equations (3) and (4). The real and imaginary parts of the dielectric constant are shown in Fig. 5. The variation of the real part follows the same pattern as the imaginary part. As expected, the values of real part are higher than that of values of the imaginary part. The real and imaginary parts of the dielectric constant increase with increasing photon energy. The real ε_1 and imaginary ε_2 parts of the dielectric constant increased from 18.60 to 32.71 and from 7.94 to 11.75 at λ = 600 nm wavelength with increasing cationic precursor concentration, respectively. These values are higher than other works [15,16].

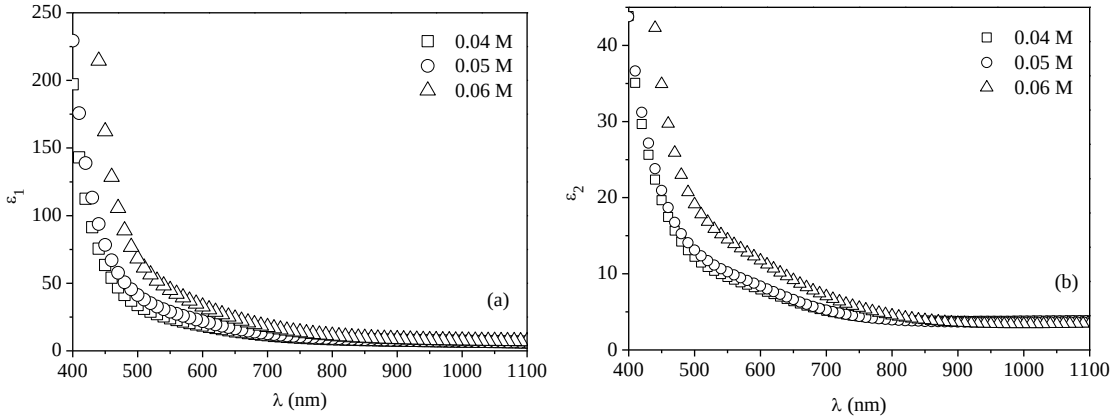


Figure 5: The dependence of the (a) real and (b) imaginary part of the dielectric constant for PbS films.

The variation of the optical absorption coefficient with wavelength was analyzed to find out the nature of the electronic transition across the optical band gap. The nature of the transition was determined using the relation:

$$\alpha h\nu = B(h\nu - E_g)^n \qquad (7)$$

where B is a constant, h is the Plank constant, ν is the frequency of photons and n equals to ½ for direct band gap [24]. Band gap E_g can be obtained by extrapolating the straight line of $(\alpha h\nu)^2$ vs. $h\nu$ curve to

intercept the horizontal $h\nu$ axis. The direct band gap E_g of the sample can be obtained as shown in Fig. 6. From this figure, it can be seen that the direct band gap of the film grown with the cationic precursor concentration decreased from 2.68 eV to 2.58 eV in table 3. This high values for the E_g of PbS films have been attributed to quantum confinement effect due to the small grain size of the polycrystalline film [19,20]. These values are consistent with the literature values of PbS thin films [21-25].

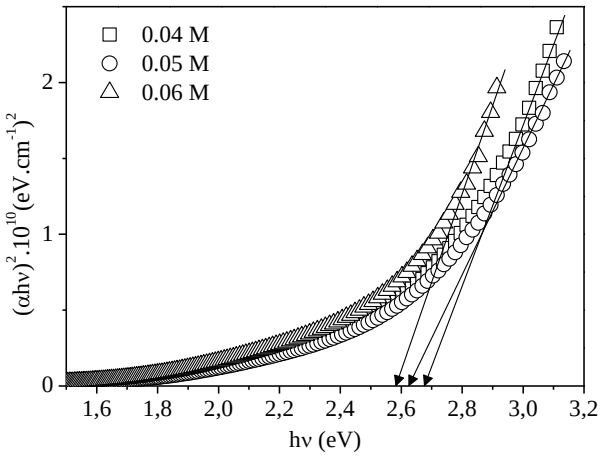


Figure 6: Plot of $(ahn)^2$ versus photon energy hn for the PbS thin films.

4. CONCLUSION

In this study, PbS thin films were prepared by successive ionic layer adsorption and reaction (SILAR) method with three different cationic precursor concentrations as 0.04 M, 0.05 M and 0.06 M on glass substrates at room temperature. XRD spectra revealed that PbS films exhibit rock salt structure of PbS. The parameter of the cubic unit cell was found to be $a \approx 0.596$ nm. Optical absorption, transmission and reflection of PbS thin films were done over the 400–1100 nm spectral region to derive the absorption coefficient, refractive index, extinction coefficient, real and imaginary part of dielectric constant. Analysis of the room-temperature absorption data revealed the existence of direct transitions in PbS films with energy band gap changing from 2.68 eV to 2.58 eV. This large optical band gap in the films is attributed to the quantum coefficient effect. It can be concluded that the structural and optical properties of the films were affected by cationic precursor concentration.

ACKNOWLEDGEMENTS

This work supported by Mehmet Akif Ersoy University Scientific Research Projects Unit under project No: 0163-YL-13.

REFERENCES

[1] F.w. Wise, Acc. Chem. Res. 33, 773 2000.
[2] T. Duan, W. Lou, X. Wang and Q. Xue, Colloid Surface A 310, 86 2007.
[3] I.e. Morales-Fernández, M.i. Medina-Montes, L.a. González, B. Gnade, M.a. Quevedo-López and R. Ramírez-Bon, Thin Solid Films 519, 512 2010.
[4] G. Konstantatos, C. Huang, L. Levina, Z. Lu and E.h. Sargent, Adv. Funct. Mater. 15, 1865 2005.
[5] J. Zhu, S.w. Liu, O. Palchik, Y. Koltypin and A. Gedanken, J. Solid State Chem. 153, 342 2000.
[6] H. Moreno-García, M.t.s. Nair and P.k. Nair, Thin Solid Films 519, 2287 2011.
[7] C.y. Wang, Y. Zhou, Y.r. Zhu, H.j. Liu and Z.y. Chen, Mater. Res. Bull. 35, 1463 2000.
[8] Y. Zhao, X.h. Liao, J.m. Hong and J.j. Zhu, Mater. Chem. Phys. 87, 149 2004.
[9] H. Wang, J.r. Zhang and J.j. Zhu, J. Cryst. Growth 233, 829 2001.
[10] K.c. Preetha, K.v. Murali, A.j. Ragina, K. Deepa and T.l. Remadevi, Curr. Appl. Phys. 12, 53 2011.
[11] A.a. Rempel, N.s. Kozhevnikova, A.j.g. Leenaers and S. Van den Berghe, J. Cryst. Growth 280, 300 2005.
[12] B. Pejova, A. Tanuševski and I. Grozdanov, J. Solid State. Chem. 177, 4785 2004.
[13] B.d. Cullity and S.R. Stock, Elements of X-ray Diffraction, Prentice- Hall, Pearson, 2001.
[14] I.J. Pankove, Optical Processes in Semiconductors, Prentice-Hall, Englewood Cliffs, NJ, 1971. (Englewood Cliffs, NJ: Prentice-Hall)
[15] M.m. Abbas, A.ab-m. Shehab, A-k. Al-Samuraee and N-a. Hassan, Energy Procedia 6, 241 2011.
[16] M.m. Abbas, A.ab-m. Shehab, N-a, Hassan and A-k. Al-Samuraee, Thin Solid Films 519, 4917 2011.
[17] J. Hernández-Borja, Y.V. Vorobiev, R. Ramírez-Bon, Sol. Energy Mater. Sol. Cells 95, 1882 2011.
[18] T. Wiktorczyk, Thin Solid Films 405, 238 2002.
[19] P.k. Ghosh, M.k. Mitra and K.k. Chatttopadhyay, Nanotechnology 16, 107 2005.
[20] R. Kostić, M. Romčević, N. Romčević, L. Klopotowski, J. Kossut, J. Kuljanin-Jakovljević, M.I. Čomor and J.m. Nedeljković, Optical Materials 30, 1177 2008.
[21] S. Kaci, A. Keffous, M. Trari, O. Fellahi, H. Menari, A. Manseri and L. Guerbous, J. Lumin. 130, 1849 2010.
[22] S. Kaci, A. Keffous, M. Trari, H. Menari, A. Manseri, B. Mahmoudi, L. Guerbous, Opt. Commun. 283, 3355 2010.
[23] S. Kaci, A. Keffous, L. Guerbous, M. Trari, Thin Solid Films 520, 79 2011.
[24] S. Kaci, A. Keffous, M. Trari, H. Menari, A. Manseri, J. Alloy. Compd. 496, 628 2010.
[25] S. Jana, R. Thapa, R. Maity, K.K. Chattopadhyay, Physica E 40, 3121 2008.